JOURNAL OF CATALYSIS 33, 434–447 (1974)

A Study of the Electron Paramagnetic Resonance and Reflectance Spectroscopy of Cobalt-Containing A, X and Y Zeolites

M. A. HEILBRON* AND J. C. VICKERMAN†

Department of Inorganic Chemistry and Catalysis, University of Technology, Eindhoven, The Netherlands

Received September 5, 1973

A study of the changes in the reflectance spectra and electron resonance (attendant upon the dehydration) of cobalt-containing zeolites revealed clear differences of behavior between zeolites A, X and Y. The data are interpreted on the basis first of the differing polarizabilities of the zeolite lattice as the Si/Al ratio is varied and second on the basis of sites available as the water content is reduced.

The location and coordination taken up by charge-balancing cations in synthetic zeolites is a problem which has been attracting increasing attention in recent years (*1–8*). A number of physical techniques have been used to tackle this problem, each one itself being unable to provide a total picture. Reflectance spectroscopy is useful in studying transition metal ions. With a sensitive detection system quite low concentrations of ions may be studied. The extinction coefficients for different coordinations (e.g., octahedral and tetrahedral Co^{2+}) are, however, rather different and thus care is required in interpretation. The EPR of Co^{2+} is very sensitive to coordination and this is in principle an attractive technique. Spin–lattice relaxation effects sometimes preclude the observation of signals especially from octahedral Co^{2+} above 4 K. Such low temperatures must necessarily affect the coordination of the cations in the zeolite especially at intermediate stages of dehydration. The present paper demonstrates that useful data can in fact be obtained at 77 K and above.

* Present address: Department of Chemical Technology, University of Twente, Enschede, The Netherlands.

† Present address: Department of Chemistry, U.M.I.S.T., P. O. Box 88, Sackville Street, Manchester, M60 1QD, England.

A detailed study of the magnetic properties of cobalt-containing zeolites (*9*) provided an outline of the variation of site occupancy by Co^{2+} as the zeolites were dehydrated. The purpose of the present study is to complement and augment those data. Reflectance spectroscopy and electron resonance have been used to make a detailed study of the influence of water content and Si/Al ratio on the cation location in synthetic zeolites.

Experimental Methods

Materials

All the samples used in the investigation were prepared from Union Carbide NaA, NaX and NaY zeolites. The Si/Al ratios of these materials are 1.00, 1.23 and 2.43, respectively. The samples were first prewashed in an acetate buffer of pH 5. Ion exchange was carried out using solutions of $Co(NO_3)_2$ of the appropriate concentration. The suspension of the zeolite in the solution was stirred for 4 hr at 80°C. The resulting zeolite was filtered out and then thoroughly washed and dried over silica gel for several days. Finally, it was stored over a saturated solution of ammonium chloride.

The cobalt content of the zeolite samples was determined by spectrophotometric analysis using a nitroso-R-salt.

The following samples were prepared and studied: CoA-70, CoA-4, CoX-3, CoX-60, CoY-80 and CoY-40 (*9*). CoA-70, etc., designates that 70% of the Na^+ ions in the parent zeolite have been exchanged for Co^{2+} ions. The diffuse reflectance and EPR spectra were studied as a function of dehydration. In general the following consecutive dehydration procedure was followed:

(I) 343 K, 1 atm dry helium, 12 hr
(II) 383 K, 1 atm helium, 12 hr
(III) 473 K, 1 atm helium, 12 hr
(IV) 573 K, 1 atm helium, 6 hr
(V) 673 K, vacuum (10^{-5} Torr), 6 hr
(VI) 773 K, vacuum, 6 hr, and
(VII) 873 K, vacuum, 6 hr.

(The Roman numerals will be used to symbolize these treatments). In some cases a vacuum procedure was used from the start. X-Ray and surface area measurements showed that the framework was still maintained after this procedure. In some cases after the last dehydration stages a study was made of the effects of adsorption of the gases N_2O, C_2H_4, H_2O and H_2S.

The diffuse reflectance spectra of the cobalt zeolites were obtained using a quartz vacuum cell fitted with an optical window. The cell was closed with a cap provided with a vacuum tap. This tap was closed when the cell was removed from the vacuum line for spectral measurements. The majority of spectra were obtained on a Pye Unicam SP800 using a SP890 diffuse reflectance accessory [wavenumber range 11.5 to 52.5 kK (1 kK = 1000 cm^{-1})] at the University of Eindhoven. Some spectra on CoX were obtained on a modified Optica Milano spectroreflectometer (10 → 50 kK) at U.M.I.S.T. A selection of the spectra have been corrected using the Kubelka–Munk equation:

$$\log[(1 - r_\infty)^2/2r_\infty] = \log k - \log s,$$

$r_\infty = R_\infty(\text{sample})/R_\infty(\text{standard})$. In most cases the standard was the Na form of the zeolite, though occasionally MgO was used. R_∞ is the reflection ratio for a thick sample and is taken as 1 for the standard; k is an absorption coefficient and s a scattering coefficient. Thus a plot of $\log\{(1-r_\infty)^2/2r_\infty\}$ as a function of wavelength gives the corrected absorption curve with a displacement due to scattering ($-\log s$).

EPR Measurements

A sample holder whose design has been described elsewhere (*10*) was used to treat the zeolite samples. The dehydration sequence followed was the same as for the reflectance measurements. Subsequent to a dehydration step, some of the sample was transferred to a quartz EPR tube which was sealed off under vacuum.

Measurements were carried out on three different EPR X-band spectrometers, a Varian E15 and an AE9 20-XT at Eindhoven and a Decca spectrometer at Manchester. In Eindhoven the magnetic field was measured using an AEG field measuring unit. The AEG and Decca cavities contained ruby crystals whose spectra were used as an intensity reference and a field calibrant.

Most measurements were made over the range of temperatures 77 to 300 K using the Varian V4540 variable temperature accessory.

Results

Host Zeolites NaA, NaX and NaY

The reflectance spectra of all the sodium zeolites were featureless in the wavelength range studied other than a weak broad band at 44 kK. The hydrated and dehydrated sodium zeolites do, however, give some weak EPR spectra. Both hydrated NaX and NaY have a weak asymmetric signal at $g = 4.3$ and a stronger symmetric resonance at $g = 2.3$ (peak to peak line width $\Delta H \sim 1200$ G). In general the NaY spectrum is more intense than the NaX spectrum. This spectrum persists through the dehydration sequence. A much less intense signal at $g = 2.2$ ($\Delta H \sim 1300$ G) is obtained from hydrated NaA. There is no evidence for the $g = 4.3$ resonance. Again this signal persists throughout the dehydration sequence. The spectra have been studied as a function of temperature and the broad $g \sim 2$ signals are ferromagnetic in character. It is known that there are iron

impurities in zeolites: McNicol and Pott (*11*) have shown that the $g = 4.3$ signal has its origin in Fe(III) in a tetrahedral environment in the zeolite lattice.

Dehydration under vacuum at 573 K or above gives rise to a sharp signal at $g = 2.0023$ ($\Delta H = 1.2$ G). This is probably due to a lattice defect. The adsorption of N_2O or C_2H_4 has a marked effect on this signal. C_2H_4 increases the intensity and N_2O decreases it.

Cobalt-Exchanged A Zeolites

i. CoA-70

Figures 1 and 2 summarize the reflectance spectra (10 kK → 30 kK) obtained for CoA-70 as a function of dehydration. The hydrated CoA-70 (i.e., CoA-70-H) gave weak bands at 15.5 kK and 19.5 kK and a shoulder at 13.0 kK. There was no EPR spectrum observed at and above 80 K for this sample. Very mild dehydration (CoA-70-I) immediately changed the sample color from pink to royal blue. A strong triplet absorption was then observed at 16.3, 17.4 and 18.5 kK with a shoulder at 21.0 kK. Concurrently an asymmetric EPR signal ($g_\perp = 5.5$, $g_\parallel = 2.05$ $\Delta H \sim 2000$ G) was detected below about 180 K. Its intensity increased with decreasing measurement temperature. The intensity of both spectra increased until dehydration IV. The triplet reflectance spectrum became broader. At dehydrations IV and V the EPR spectrum decayed rapidly and the reflectance spectra triplet maxima shifted to about 15.7, 16.9 and 19.5 kK with a shoulder at 24 kK. This spectrum was sensitive to the adsorption of N_2O, C_2H_4 and H_2 (Fig. 2). Further dehydration at 770 K and 870 K (i.e., VI and VII) gave rise to three separate bands at 14.8, 16.8 and 19.5 kK. After dehydration at 870 K a new EPR signal also appears at room temperature at $g_\perp = 2.05$ and $g_\parallel = 3.6 (g_{av} = 2.4)$ and $\Delta H = 1700$ G (Fig. 3). The signal intensitv *decreases* with decreasing temperature. These spectra are not sensitive to N_2O at 300 K but exposure to H_2O vapor causes both spectra to revert to the dehydration II condition. The fully hydrated zeolite condition cannot be restored

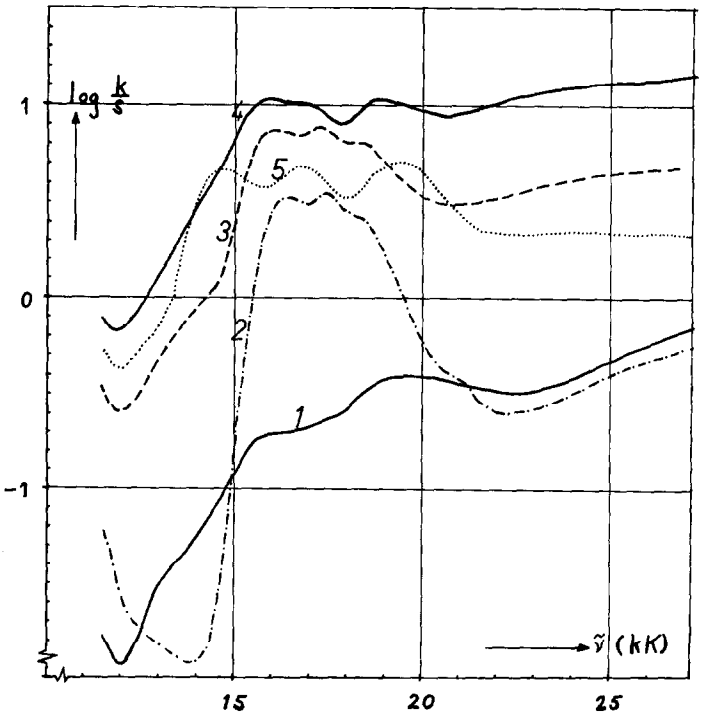

FIG. 1. The reflectance spectra of the dehydration of CoA-70: (1) hydrated CoA-70; (2) dehydration I; (3) dehydration III; (4) dehydration IV; (5) dehydration VII.

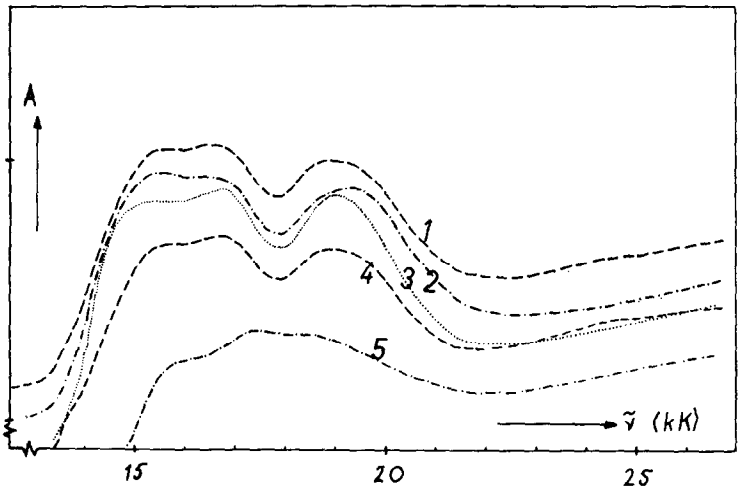

FIG. 2. Adsorption effects at room temperature after dehydration V of CoA-70. Between each adsorption the sample was outgassed at 673 K: (1) dehydration V; (2) after N_2O adsorption; (3) after C_2H_4 adsorption; (4) after H_2 adsorption; (5) after H_2O adsorption. Spectra 2, 3 and 4 have been displaced downwards in the interests of clarity.

even after prolonged exposure to H_2O vapor. It is interesting to note that even when CoA zeolite is suspended in water the blue coloration and dehydration II spectrum can be obtained when the temperature of the water is raised to 333 K. The zeolite returns to its pink color very slowly over a period of several days.

ii. CoA-4

The dehydration sequence gave broadly similar results though the blue coloration and triplet spectrum were not obtained until dehydration III. This triplet (at 15.6, 17.1 and 18.7 kK) however, was that obtained at stage V in CoA-70 and this may explain why no EPR signal could be detected until dehydration VII. This signal having $g_{av} = 2.6$ and $\Delta H \sim 1500$ G was similar to that obtained in CoA-70 at this dehydration.

Cobalt-Exchanged Y Zeolites

i. CoY-80 and CoY-40

The reflectance spectra for the dehydration sequence on these samples are shown in Figs. 4 and 5. Hydrated CoY gives two weak bands at ~14.0 and 19.5 kK. At dehydration III a triplet absorption is first observed at about 15.1, 17.2 and 18.5 kK. The intensity rises at dehydration IV but thereafter there is a marked fall with the development of a band at 13.5 kK and a shoulder at ~14.6 kK at dehydrations VI and VII. It is only at these latter stages that an EPR signal appears having $g_{av} = 2.4$ and $\Delta H \sim 1000$ G (Fig. 3). The signal intensity decreases with decreasing temperature. After dehydration VII, adsorption at room temperature of C_2H_4 tends to increase the EPR signal and restore the triplet absorption (Fig. 5) while N_2O decreases the EPR signal. H_2 and O_2 adsorption at 25°C has little effect on the spectra.

H_2S adsorption at 25°C caused the sample to turn black. The reflectance spectrum had a single intense band at 33 kK. Heating the sample at 400°C in O_2 restored the triplet of dehydration III and destroyed the EPR signal.

Room temperature adsorption of H_2O vapor restored the reflectance spectrum obtained for the fully hydrated CoY. The EPR signal was destroyed.

ii. CoY-1.5

The spectral observations were similar to those above except that at no stage was an EPR signal detected.

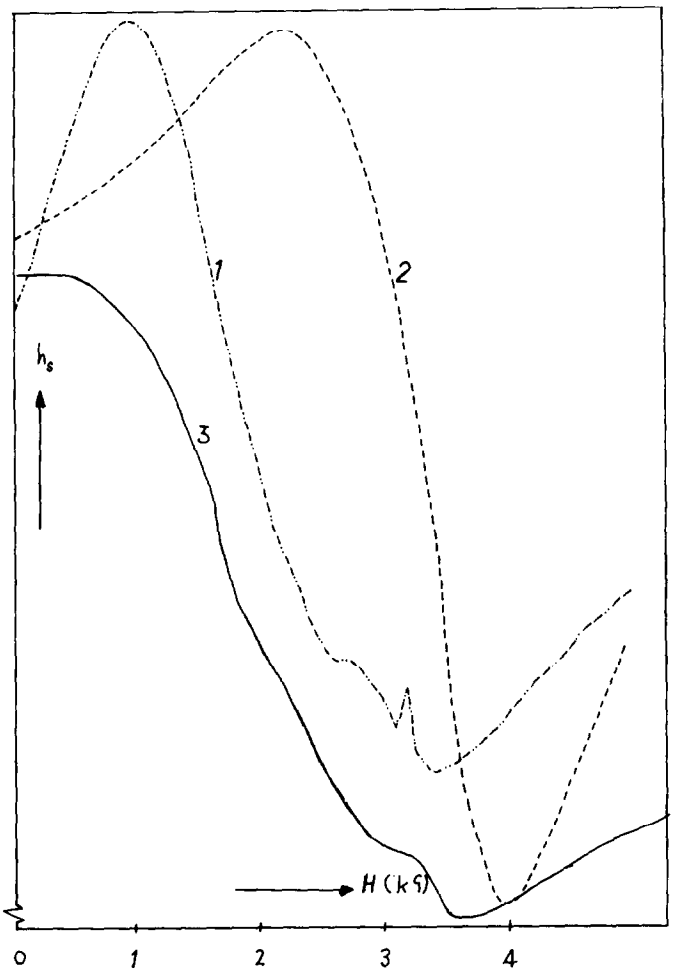

FIG. 3. Some X-band EPR signals from CoA-70 and CoX-60: (1) CoA-70 after dehydration II, measuring temperature 220 K. (2) CoA-70 after dehydration VII, measuring temperature 300 K. (3) CoX-60 after dehydration VII, measuring temperature 100 K.

Cobalt-Exchanged X-Zeolites

i. CoX-60

The dehydration sequence gave rise to reflectance spectra similar to those shown in Fig. 6 for CoX-3. The hydrated CoX-50 gave a spectrum similar to hydrated CoY with bands at 14.4, 19.1 and 20.2 kK. Dehydration II gave rise to a strong triplet similar to that observed in CoA with maxima at about 16.1, 17.4 and 18.5 kK and a shoulder at 20.8 kK. At this stage an EPR signal appeared at $T < 220$ K having $g_\perp \sim 5.6$ and $g \sim 2.08$ and a peak to peak width of about 2000 G. The signal intensity increased with decreasing temperature to 90 K.

At the following two dehydration stages (III and IV) the EPR signal decreased and the reflectance maxima shifted and decreased. At dehydration V the EPR signal had disappeared even at 90 K, although there was a new weak room temperature resonance. The reflectance spectra at this stage had a maximum at 13.8, a triplet set of maxima at 15.2, 17.2, 18.7 and a shoulder at 20.5 kK.

Dehydration VI gave rise to two new EPR signals at room temperature. One signal had $g_\parallel \sim 3.3$, $g_\perp \sim 2.1$ and a width

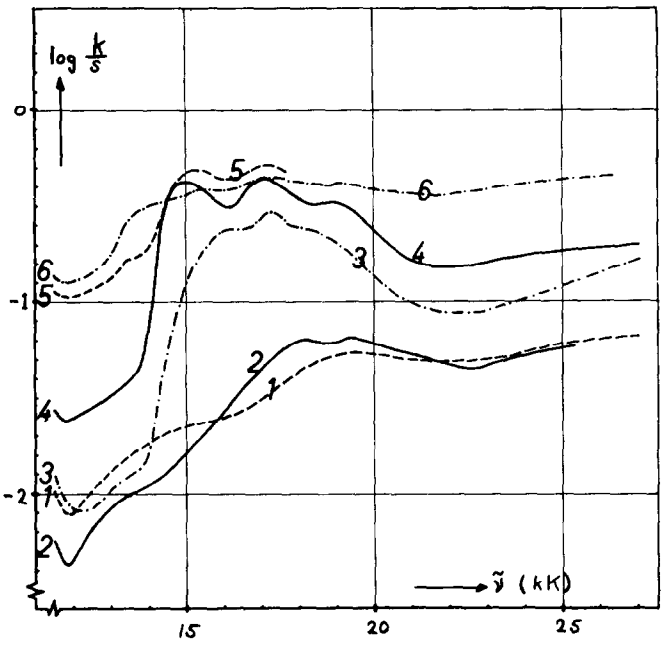

FIG. 4. Reflectance spectra of the dehydration of CoY-50: (1) hydrated; (2) dehydration II; (3) dehydration III; (4) dehydration IV; (5) dehydration V, (6) dehydration VII.

of ~1500 G. This signal decreased with decreasing measuring temperature. The other was very sharp ($\Delta H \sim 10$ G) and occurred at $g = 1.90$. At 100 K a new, very broad but very intense signal replaced it having $g_\perp > 6$ and $g_\parallel \sim 2$ (Fig. 3). This signal was not visible at room temperature. Further evacuation at 870 K increased the intensity of this broad signal and removed the $g_\parallel \sim 3.3$, $g_\perp$ 2.1 signal.

Room temperature adsorption of H_2O vapor destroyed this EPR signal and caused a gradual restoration of the hydrated CoX-60 reflectance spectrum.

ii. CoX-3

The dehydration sequence gave a similar set of reflectance spectra to CoX-60. The intensities, of course, were much lower. Slight dehydration gave rise to the 16.2, 17.3 and 18.5 kK triplet. Further dehydration again shifted the maxima to 15.8, 17.1 and 18.6 kK. This was accompanied by the appearance of an EPR signal below 220 K. In this case it was narrower than for CoX-60; $g_\perp = 4.4$, $g_\parallel = 4.09$ and $\Delta H = 1129$. Dehydrations IV and V caused a decrease in this signal. The reflectance spectra revealed a concomitant development of a band at 13.5 kK and a shift in the triplet maxima to 15.0, 17.1 and 18.9 kK. At dehydration VI, unlike CoX-60 there was no room temperature EPR spectrum at $g = 2.11$ or a spectrum at 100 K, but the sharp signal at $g = 1.90$ did appear. The reflectance spectrum, however, was similar to CoX-60.

DISCUSSION

In seeking to elucidate the Co^{2+} ion environments found in zeolites which give rise to the observed spectra it is first necessary to discuss the structural contrast between A, X and Y zeolites.

The zeolites A, X and Y can be considered as consisting of a 3-dimensional arrangement of six-membered rings of Al and Si connected oxygen atoms. For example, eight such rings are combined to form the sodalite unit (or β-cages). The difference between the three zeolite structures lies in the manner in which these sodalite units are combined.

The Si/Al ratio in A zeolite is 1.00. Hence the six-membered ring will have the form

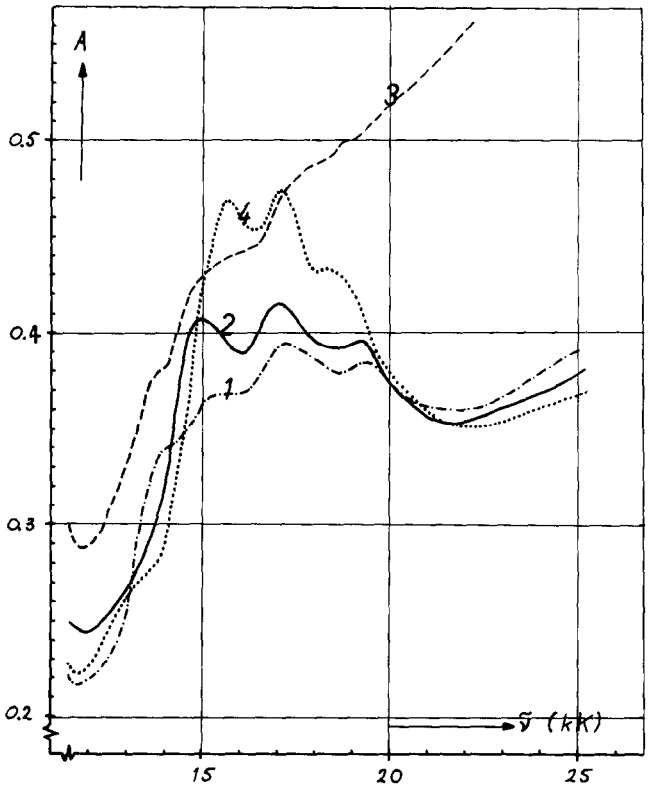

FIG. 5. Adsorption effects on CoY-50 after dehydration VII. Between each adsorption the sample was outgassed at 873 K: (1) dehydration VII; (2) C_2H_4 adsorption at 300 K; (3) H_2S adsorption at 300 K; (4) O_2 adsorption at 680 K.

(the Al–O–Al combination is forbidden):

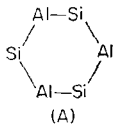

In X and Y zeolites the Si/Al ratio is between 1 and 3. Thus, in addition to (A) rings, the following six-membered rings are also theoretically possible:

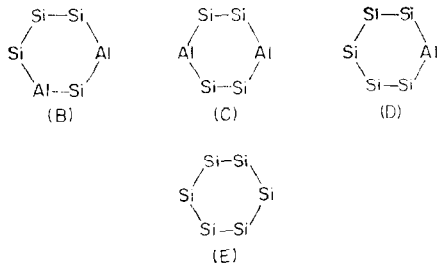

X-Zeolite has a Si/Al ratio of 1.23. If the Al and Si distribution is homogeneous it is probable that (A) and (B) rings predominate. The unit cell is Na_{86} $(AlO_2)_{86}$ $(SiO_2)_{106}$ 264 H_2O. This would imply six sodalite cages with 11 Al^{3+} and two with 10 Al^{3+}. Thus there would be 44(A) and 20(B) rings or possibly 44(A), 16(B) and 4(C) rings, though (C) rings impose restrictions on the linking of sodalite units since (A) and (C) rings cannot link. If an inhomogeneous distribution of Al^{3+} is assumed then many more configurations become possible.

Y-Zeolite has a Si/Al ratio of 2.43. The (B), (C), (D) and (E) rings become more likely. If (E) rings are unlikely, then for a homogeneous Al^{3+} distribution each sodalite unit will consist of six (B) or (C) rings and two (D) rings. The highest Si/Al ratio in zeolites is three and in this case four (B)

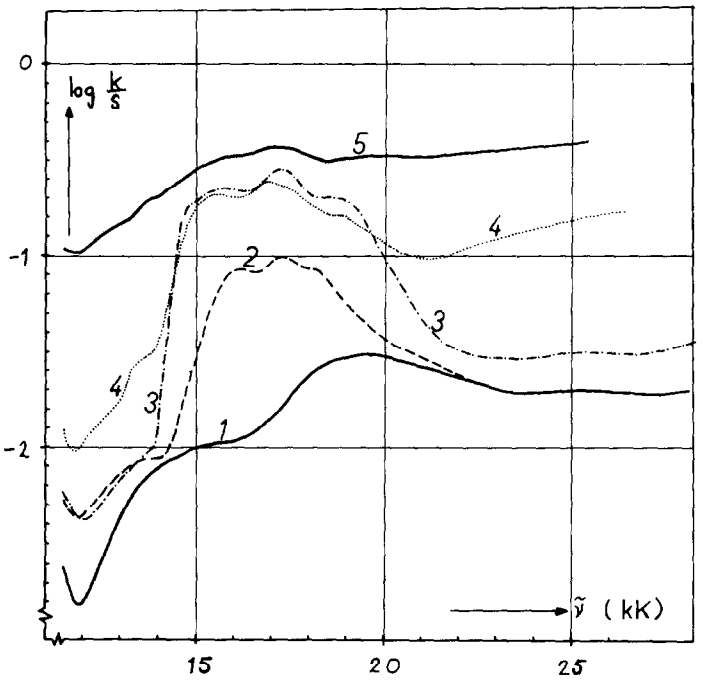

FIG. 6. Reflectance spectra of the dehydration of CoX-3: (1) hydrated; (2) dehydration I; (3) dehydration II; (4) dehydration IV; (5) dehydration VII.

or (C) rings and four (D) rings would be expected in each sodalite unit.

An (A) type ring has three Al^{3+} per ring and can be considered to have an effective charge of 3−. (B) and (C) rings will have a charge of 2− and (D) rings of 1−. Charge-balancing cations might be expected to be more strongly bonded to (A) rings than to (B), (C) and (D) rings. Thus cations bonded to (A) rings will have a lower effective charge than cations bonded to (B), (C) and (D) rings.

As Dempsey and Olson (*12*) have suggested, the interaction of cations with the A and X zeolite frameworks might be expected to differ from that with Y zeolites. The spectral data in Table 1 for the dehydrated zeolites suggests that this is in fact true. The details will now be considered.

The Hydrated Zeolites

In an ideal octahedral environment the ground state of high spin Co^{2+} is $^4T_{1g}(F)$ with $S = 3/2$. Spin–orbit coupling removes the degeneracy of this state so that the effective spin will be $S' = \frac{1}{2}$. The reflectance spectra of hydrated CoX-3, CoX-60, CoY-1.5, CoY-40 and CoY-80 are all the same. Fitting the observed bands in the Tanabe-Sugano diagram results in $Dq = 730$ cm^{-1} and $B = 890$ cm^{-1}. The band positions for CoA-70 are somewhat different and they result in $Dq = 870$ cm^{-1} and $B = 840$ cm^{-1}. It is normal to calculate Dq and B from the $^4T_{1g}(F)$ to $^4T_{2g}(F)$ and $^4T_{1g}(P)$ transitions using the $^4A_{2g}(F)$ level as a check. In the present case information is only available on the $^4T_{1g}(P)$ and $^4A_{2g}(F)$ transitions. Thus the calculations are subject to some uncertainty. Nevertheless, the higher Dq/B ratio for A zeolites is confirmed by the appearance of the weak $^2T_1(G)$ or $^2T_2(G)$ band at 13.0 kK.

If in all three zeolites the Co^{2+} ions were tumbling in the zeolitic water in the supercages it would be expected that Dq, and probably B, would be the same for all three. The high Dq value for the A zeolite suggests that the strong electric field due to the (A) rings in the zeolite framework is influencing the crystal field of the Co^{2+} ion. This would imply that the Co^{2+} ions are

TABLE 1

Dehydration stage (subscript refers to sample)		Reflectance spectra: Data in kK (assignments below where possible)								Notes	EPR spectra: g-values	Temp behavior	Notes
H_A	H	13.0 $^2T_{1g} + {}^2T_{2g}$(G)		15.5 $^4A_2$ (F)			19.5 $^4T_{1}$(P)		32				No spectra evident above −180°C
H_{XY}	H		14.0 $^4A_{2g}$(F)				19.5 $^4T_{1g}$(P)	20.6	30		$g_\perp \sim 26$–9 $g_\parallel \sim 2$ $g_{av} = 3.4$	Increase with decr. temp	Spectra evident below −180°C
II_Y	110°C He	11.7				18		20.5					Spectra evident below −180°C
II_{AX}	110°C He				16.3 $^2T_1$(G)	17.4 $^4T_1$(P)	18.5 $^2T_2$(G)	21.0 $^2T_1$(P)	32 47		$g_\perp = 5.5$ $g_\parallel = 2.05$	Increase with decr. temp $T \leq$ −50°C	Dilute samples $g_\perp = 4.4$ $g_\parallel = 4.09$
III_Y	200°C He			15.9		17.3	18.7	20.7	35 47				No spectra evident at $T \geq$ −180°C

IV_{AX}	300°C He			15.7 $^2T_1$(G)		17.1 $^4T_1$(P)	18.6 $^2T_2$(G)		20.8	35	47	$IV_{AX} \sim III_Y$	(i) $g_\perp = 5.5$ $g_\parallel = 2.05$	As for II_{AX}	Intensity low relative to II_{AX}
									24.0				(ii) $g_{av} = 2.2$	As VII_A	Low relative to VII_A
V_A	400°C Vac.			15.7	16.8			19.5	24	35	47	$V_A = IV_{AX} + VII_A$	(i) $g_\perp = 5.5$ $g_\parallel = 2.05$		III_{AX} very weak
													(ii) $g \sim 3.3$ $g \sim 2.1$		VII_A developing but weak
V_{XY}	400°C Vac.	13.5 (weak)		15.0		17.1	18.9			35	47	$V_{XY} \sim VII_A$	$g_{av} = 2.2$ for X ~ 2.1	Decrease with decr. temp	Weak signal similar to VII_A
VII_A	600°C Vac.			14.8	16.8			19.5	26	35	47		$g_\parallel \sim 3.3$ $g_\perp \sim 2.1$ $g_{av} = 2.2$	Decrease with decr. temp	Observable at 25°C
VII_Y	600°C Vac.	13.5		15.4		17.1	18.9		21	35	45	$VII_Y = V_Y + VII_X$	$g_\parallel \sim 3.3$ $g_\perp \sim 2.1$ $g_{av} = 2.2$	Decrease with decr. temp	Observable at 25°C
VII_X	600°C	13.8	14.6					19.8		30	45	$VII_X \sim H_{XY}$	$g_\perp \sim 36$ $g_\parallel \sim 2$	Increase with decr. temp	Observable below −170°C

located close to the zeolite walls. That this is not true for X-zeolites is probably due to the much higher H_2O/Co ratio in X than in A; hence X maintains a fully hydrated Co^{2+} species. Furthermore, B for the A zeolite is lower than for X and Y. This low value can be interpreted as implying a greater delocalization of the electron cloud of Co^{2+} in A than in X or Y, again suggesting some interaction of the Co^{2+} electron cloud with framework oxygen ions. Additionally, the lower B value may be partly due to compression of the water ligands around the Co^{2+} ions in the hexagonal windows due to the geometry of the A zeolite structure. The B value of the free Co^{2+} ion is 980 cm^{-1} (*13*) whereas in MgO it is 810 cm^{-1} (*14*). In aqueous solutions, however, $B = 883$ cm^{-1} (*15*). These data further suggest that in the X and Y zeolites the Co^{2+} ions are relatively free as $Co^{2+}(H_2O)_6$ species, but in A zeolite there is probably an interaction with the zeolite framework.

Comparison of the magnetic data for hydrated CoA-70 and CoY-50 (*9*) revealed some marked differences. The reciprocal susceptibility curve for CoA-70 rises above that for CoY-50 (and the theoretical curve for octahedral Co^{2+}), implying a reduction in the orbital contribution to the susceptibility. The EPR data for CoY are masked by the strong Fe^{3+} impurity signal from the Y lattice, but at 90 K CoX-60 has a strong EPR signal whereas CoA-70 does not. A small increase in the spin–lattice relaxation time due to a modification of orbital energy levels could account for this. Both these observations are consistent with a distorted octahedral environment of ligands around the majority of Co^{2+} in A zeolite due probably to a species of the type $Co(Ox)_3(H_2O)_3$, whereas in X and Y the majority of Co^{2+} ions are in a more symmetrical octahedral field of the type $Co^{2+}(H_2O)_6$.

The Octahedral-Tetrahedral Transition

As the zeolites are dehydrated, the H_2O/Co ratio decreases and tetrahedral and lower symmetries become likely. A characteristically tetrahedral spectrum is produced under very mild dehydration conditions (I) in CoA-70, CoA-1, CoX-60 and CoX-3, while much stronger conditions (III) are required for the CoY zeolites. The details of the spectra are discussed below. Suffice it to say at present that the spectrum is very similar to that assigned to $[Co(OH)_3H_2O]$ (*15*).

In the last section it was suggested that in CoA most of the Co^{2+} ions are situated in the hexagonal windows (site II) where they bind with three lattice oxygens and three water ligands. In this position the following equilibrium can take place:

$$Co(Ox)_3(H_2O)_3(\text{pink}) \rightleftharpoons Co(Ox)_3H_2O(\text{blue}) + 2H_2O$$

This occurs at the first stage of dehydration for CoA when the ratio of H_2O/Co is above six. In hydrated CoX and CoY, $Co^{2+}(H_2O)_6$ has been suggested as the majority species. A tetrahedral species occurs at an early stage in CoX when the H_2O/Co ratio is above six, whereas with CoY-80 it does not occur until the H_2O/Co ratio reaches about four at dehydration III (*9*). This difference between A and X on the one hand and Y zeolite on the other can be understood when it is remembered that unlike Y, A and X have a predominance of type (A) rings. As in the case of hydrated CoA, these rings with their three negative charges will attract the Co^{2+} ions strongly in the X zeolite as the water content falls. Thus in A and X zeolites the Co^{2+} ions may be polarized close to the zeolite framework forming a species $Co^{2+}(Ox)_3$ having an effective charge close to one negative charge. Such a species will not attract water ligands very strongly and thus a ready transition to $Co(Ox)_3H_2O$ having an elongated tetrahedral symmetry (probably in site II) is not surprising.

In Y zeolites, however, (B) and (C) rings predominate. They will not attract the Co^{2+} ions so strongly. This, combined with the fact that in Y zeolites the H_2O/cation ratio at a given water content is higher than in A or X, makes polarization of the Co^{2+} ions at the zeolite wall less likely at this stage of dehydration. Furthermore, it was pointed out earlier that the tetrahedral species found in CoY is not obtained until the

H_2O/Co ratio ≤ 4, suggesting a smooth transition from $Co^{2+}(H_2O)_6$ to $Co^{2+}(H_2O)_4$ as H_2O is removed. This suggestion is supported by the CoY-80 spectrum for dehydration II which can be attributed to 5-coordinate Co^{2+} (*16*). Alternatively, if as H_2O is removed Co^{2+} ions are adsorbed on the walls of Y zeolite, it can be argued that the Co^{2+} ions will be less closely bonded to the walls than in A or X. The charge on the $Co(Ox)_3$ species so formed would be 0, +1 or higher. Thus H_2O ligands will be more strongly held than in A or X. This would explain (a) why a five-coordinate species appears to be present, (b) why the four-coordinate species appears at such low H_2O/Co ratios, and (c) why an EPR signal is not observed for the tetrahedral species, since the Co^{2+} will be in a less distorted crystal field than in X or A.

Further support for these arguments arises from a consideration of the details of the reflectance and ESR spectra for dehydrations II and III.

In an ideal tetrahedral complex the ground state of Co^{2+} is $^4A_2$ with $S' = 3/2$. There are two spin and orbitally allowed transitions to $^4T_1(F)$ and $^4T_1(P)$, one solely spin allowed transition to $^4T_2(F)$, four solely orbitally allowed transitions to the $^2T_1(G)$, $^2T_1(P)$ and two $^2T_1(H)$ levels, and many others that are both spin and orbitally forbidden. In the spectral region studied, the only completely allowed transition to the $^4T_1(P)$ level produced a very strong band in the 17 kK region. The partly forbidden transitions to $^2T_1(G)$ and $^2T_2(G)$ are also visible, though less intense. Utilizing these transitions, very approximate values of Dq and B can be obtained from the Tanabe-Sugano diagram.

Spectrum II_{AX} (see Fig. 6 and Table 1) is very sharp and the position of the $^4T_1(P)$ transition is higher than is usual (*14*, *17*, *18*) resulting in $Dq \sim 410$–420 cm^{-1} and $B \sim 800$ cm^{-1}. Associated with this spectrum was an EPR signal having $g_\perp \sim 5.5$ and $g_\parallel \sim 2.0$. This signal was not visible at room temperature but its intensity rose rapidly with decreasing temperature. It is consistent with Co^{2+} in an elongated tetrahedral environment (*8*). The spin–lattice relaxation time of tetrahedral Co^{2+} complexes is very sensitive to the orbital contribution. In cubic environments the first excited state is a T state which often means that very low temperatures are required to detect the signal. Distorted tetrahedral environments split the T state such that the first excited state is an E level or in some cases an A level, thus lowering the orbital contribution and raising the temperature of detectability.

With further dehydration of A and X zeolites this EPR signal decreases and the reflectance spectra maxima shift to lower energies such that IV_{AX} and III (see Table 1) are similar. A rough estimate suggests that $Dq \sim 400$ cm^{-1} and $B \sim 800$ cm^{-1}. The species is clearly tetrahedral and is almost identical to that observed by us for Co^{2+} in γ-Al_2O_3 (*19*) where the tetrahedral sites are essentially undistorted. In this example no EPR signal is visible above 90 K. At dehydrations III to IV the H_2O/Co ratio for CoA-70, CoY-80 and CoX-60 has fallen from 2 to 1. The supercage water will be almost completely desorbed, and most of the water which remains will be retained in the sodalite units. Movement of the cobalt ions into the sodalite units is to be expected, taking up positions in sites I′ or II′. Spatial and electrostatic considerations will cause tetrahedral species to be more compressed than is possible in site II. Thus a transition to an almost undistorted tetrahedral $Co(Ox)_3H_2O$ species in Site I′ or II′ may be expected for CoX and CoA. Thus it is suggested that the tetrahedral Co^{2+} species [$Co(H_2O)_4$ or $Co(Ox)_3$ H_2O and then $Co(Ox)_3OH$] in CoY are always approximately cubic, whereas the tetrahedral species in A and X are first distorted [$Co(Ox)_3H_2O$] in site II and then become more cubic in site I′ or II′. This is in line with the magnetic susceptibility data for CoA and CoY in this zone of dehydration (*9*). The Y samples rise to a χ^{-1} plateau for the tetrahedral species. In CoA there is a rise in χ^{-1} to dehydration II followed by a marked fall to dehydration IV, suggesting a transition from a species having a low

orbital contribution to the susceptibility to one having a higher contribution.

The Final Stages of Dehydration

Dehydration of the CoA specimens at 670 and 870 K in vacuum results in new reflectance and EPR spectra. The reflectance spectrum consists of three equally intense bands. This spectrum is rather unusual but can be attributed to Co^{2+} in a compressed tetrahedral environment (*8*) [$Co(Ox)_3OH^-$ or $Co(Ox)_3O^{2-}$ in site I′ or II′], or trigonal [in site I′ or II′].Such an environment would be expected to give rise to a zero field splitting parameter (D) less than zero. If this parameter is large (~ -10 cm^{-1}) a transition within the $\pm\frac{1}{2}$ doublet would only be expected to appear when its population becomes appreciable; hence the apparent increase of intensity with increasing temperature. Due to the breadth of this signal an accurate quantitative estimate of the variation of intensity with temperature cannot be made, though it is possible to say that the intensity increases to about 300 K and then remains approximately constant as the line width narrows.

Another possible explanation of the observed temperature behavior of the ESR signal is that the Co^{2+} ions form exchange coupled pairs. A signal would only appear above the temperature where $J/kT \sim 1$ (J is the exchange integral). The magnetic data do not show any real evidence of exchange effects (*9*). The susceptibility curve follows the theoretical tetrahedral line very closely with a Weiss constant of zero. Thus the former explanation appears more reasonable. A pure trigonal environment is also rather unlikely since it would be very difficult to remove the last water fragments, OH^- or O^{2-}.

In the X and Y zeolites there is evidence of the VII_A reflectance spectrum and the EPR spectrum is certainly evident, showing that a similar species is present in these zeolites. However, there are further spectral features particularly clearly seen in VII_X. The reflectance spectrum is easily attributable to octahedral Co^{2+} since it is very similar to H_{XY}. Furthermore an EPR signal appears below 100 K which is clearly similar to H_{XY} and due to octahedral Co^{2+}. Such features can only arise from Co^{2+} in the hexagonal prisms [$Co(Ox)_6$, site I].

That a proportion of the Co^{2+} ions have gone into site I in the CoY samples is evident from III_Y which is a composite of V_Y and VII_X. This observation is in clear agree-

TABLE 2

Dehydration stage	Assignment of cobalt species observed		
	A	X	Y
H	$Co(Ox)_3(H_2O)_3$ site II	$Co(H_2O)_6$	$Co(H_2O)_6$
II	$Co(Ox)_3H_2O$ site II	$Co(Ox)_3H_2O$ site II	$Co(H_2O)_5$
III & IV	$Co(Ox)_3H_2O$ site I′ or II′	$Co(Ox)_3H_2O$ site I′ or II′	$Co(H_2O)_4$ + $Co(Ox)_3H_2O$ site II
V	$Co(Ox)_3OH^-$ or $Co(Ox)_3O^{2-}$ site I′ or II′	$Co(Ox)_3OH^-$ or $Co(Ox)_3O^{2-}$ site I′ or II′	$Co(Ox)_3OH^-$ or $Co(Ox)_3O^{2-}$ site I′ or II′
VII	$Co(Ox)_3OH^-$ or $Co(Ox)_3O^{2-}$ site I′ or II′	$Co(Ox)_3O^{2-}$ site I′ or II′ + $Co(Ox)_6$ site I	$Co(Ox)_3O^{2-}$ site I′ or II′ + $Co(Ox)_6$ site I

ment with the susceptibility measurements (*9*), where χ^{-1} dropped sharply at the final dehydration. In conclusion, Table 2 summarizes the dehydration sequences which appear to be in accord with these data and with the earlier magnetic study (*9*).

Adsorption Effects

N_2O, C_2H_4 and H_2O adsorptions were studied at dehydrations V and VII. At dehydration V, N_2O adsorption tended to produce a reflectance spectrum characteristic of dehydration VI, whereas C_2H_4 produced a reflectance and EPR spectrum characteristic of dehydration III. C_2H_4 had a similar effect at dehydration VII. This suggests that C_2H_4 may be able to cause Co^{2+} to migrate out to the supercages to form a $Co(Ox)_3$ C_2H_4 species in site II. N_2O, on the other hand, had little effect at dehydration VII, but heating at 200°C produced a weak EPR signal characteristic of dehydration II. Movement out of the sodalite units to adsorb and/or decompose N_2O may occur at elevated temperatures.

H_2O adsorption on both V and VII samples of A, X and Y first rapidly produces spectrum IV_{AXY}. After a long exposure to H_2O vapor the final spectrum for A and X is II_{AX} but for Y it is H_{XY}. It would seem that it is difficult to remove Co^{2+} ions from site I′ or II′ in A and X zeolites once the dehydration procedure has caused them to migrate there. This is probably due to the predominance of (A) rings in these zeolites.

Acknowledgments

The authors acknowledge the help and encouragement given by Professor G.C.A. Schuit and the award of a Royal Society European Fellowship to one of us (J.C.V.).

References

1. Egerton, T. A., and Stone, F. S., *J. Chem. Soc. Faraday I* **69**, 22 (1973).
2. Olson, D. H., *J. Phys. Chem.* **72**, 4366 (1969).
3. Gallezot, P., Ben Taarit, Y., and Imelik, B., *J. Catal.* **26**, 481 (1972).
4. Barry, T. I., and Lay, L. A., *J. Phys. Chem. Solids* **29**, 1395 (1968).
5. Slot, H. B., and Verbeek, J. L., *J. Catal.* **12**, 2116 (1968).
6. Klier, K., and Ralek, M., *J. Phys. Chem. Solids* **29**, 95 (1968).
7. Klier, K., *J. Amer. Chem. Soc.* **91**, 9392 (1969).
8. Mikheikin, I. D., Brotikovskii, O. I., Zhidomirov, G. M., and Kazanskii, V. B., *Kinet. Katal.* **12**, 1442 (1971).
9. Egerton, T. A., Hagan, A., Stone, F. S., and Vickerman, J. C., *J. Chem. Soc. Faraday I* **68**, 723 (1972).
10. Cornaz, P. F., Van Hooff, J. H. C., Pluijm, F. J., and Schuit, G. C. A., *Discuss. Faraday Soc.* **41**, 290 (1966).
11. McNicol, B. D., and Pott, G. T., *Chem. Commun.* 438 (1970).
12. Dempsey, E., and Olson, D. H., *Phys. Chem.* **74**, 305 (1970).
13. Griffiths, J. S., "The Theory of Transition Metal Ions," Cambridge University Press, London, 1961.
14. Reinen, D., *Struct. Bonding (Berlin)* **7**, 114 (1970).
15. Hathaway, B. J., and Lewis, C. E., *J. Chem. Soc., Ser. A* 1183 (1969).
16. Ciampolini, M., *Struct. Bonding (Berlin)* **6**, 52 (1969).
17. Ferguson, J., Wood, D. L., and Van Uitect, L. G., *J. Chem. Phys.* **51**, 2904 (1969).
18. Pappalardo, R., Wood, D. L., and Linares, R. C., *J. Chem. Phys.* **35**, 2041 (1969).
19. Heilbron, M. A., thesis, Eindhoven, 1971.